Ionicity of nickel oxide: Direct determination by reflection diffraction of high-energy electrons from the (100) surface

L.-M. Peng
Beijing Laboratory of Electron Microscopy, Institute of Physics and Center for Condensed Matter Physics, Chinese Academy of Sciences, P.O. Box 2724, Beijing 100080, People's Republic of China

S. L. Dudarev and M. J. Whelan
Department of Materials, University of Oxford, Parks Road, Oxford OX1 3PH, United Kingdom
(Received 20 June 1997; revised manuscript received 18 August 1997)

The degree of ionicity and the inner potential of crystalline nickel oxide have been determined by using reflection high-energy electron diffraction (RHEED) and reflection electron microscopy. By matching experimental RHEED patterns obtained from an atomically flat NiO(100) surface with dynamical RHEED calculations, we found that the degree of ionicity of this oxide is close to 0.3, and that the inner potential equals 21.21 V. [S0163-1829(97)08644-X]

I. INTRODUCTION

In recent years transition-metal compounds (TMC's) and their surfaces have attracted considerable attention both in view of potential practical application of these compounds in catalysis,[1–3] and also because of their highly unusual electronic properties resulting from the presence of strong electron-electron correlations in the *d* shell of metal ions.[4,5] Nickel oxide is a typical example of a TMC, and its bulk electronic structure[6–8] as well as the electronic structure of its (100) surface[9,10] currently remains the subject of much debate.

The existing approaches to electronic and mechanical properties of nickel oxide are often based on contradictory assumptions. For example, shell-model interatomic potentials of NiO,[11] giving accurate description of phonon-dispersion curves, are based on the assumption that chemical bonding in NiO is entirely ionic. At the same time it is known that *neutral-atom* rather than ionic charge densities provide the best starting point for a self-consistent electronic-structure calculation.[12] It is also known that the effective crystal potential constructed using *neutral-atom* charge densities makes it possible to reproduce well the spectrum of one-electron excitations of NiO.[13]

The question about the form of representation of the crystal potential becomes particularly important for interpreting experimental data on surface properties of this oxide. For example, understanding of the origin of the mechanism responsible for the formation of crosslike scanning tunneling microscopy images of defects,[9] and the $c(2\times2)$ reconstruction observed in *empty* electronic states near step edges requires evaluation of charge density and electrostatic potential both in the bulk crystal and in the vacuum region above the surface.

In this paper, we show how the degree of ionicity of nickel oxide *and* its electrostatic potential can be determined using high-energy electron diffraction. Diffraction intensities are known to be highly sensitive to the distribution of charge in the unit cell,[14] and below we demonstrate how a combination of reflection high-energy electron diffraction (RHEED) and reflection electron microscopy (REM) makes it possible to determine both the degree of ionicity of nickel oxide and the inner potential of the crystal.

The degree of ionicity α can be defined in the following way:

$$f(s)=(1-\alpha)f_{\text{neutral}}(s)+\alpha f_{\text{ion}}(s), \tag{1}$$

in which $f_{\text{neutral}}(s)$ and $f_{\text{ion}}(s)$ denote scattering factors of neutral atoms, such as Ni or O, and of their ions, Ni^{2+} or O^{2-}, respectively, and $f(s)$ denotes the scattering factor associated with the resulting distribution of charge around a particuar lattice site in a crystal. RHEED intensities depend on the crystal potential $V(\mathbf{r})$, which in turn depends primarily on the atomic scattering factor $f(s)$ and therefore on the ionicity α via Eq. (1). The degree of ionicity α may thus be obtained by fitting an experimental RHEED pattern with the results of calculations.

The inner potential of the crystal is closely related to its ionicity. Once the ionicity α is determined, the crystal inner potential may then be obtained using the formula

$$V_0=\frac{\hbar^2}{2m_0e}\cdot\frac{4\pi}{\Omega}\lim_{s\to0}\sum_i f_i(s), \tag{2}$$

where Ω is the volume of a bulk unit cell of the crystal, e is the electron charge, and the summation goes over all atoms within a unit cell.

Accurate measurement of the crystal inner potential using the technique of electron diffraction has been a subject of intensive investigations since the early days of electron diffraction,[15,16] and this subject has been recently reviewed by Spence[17] and O'Keeffe and Spence.[18] The interest in this subject results mainly from two points. First, the crystal inner potential is directly proportional to the second moment of

the charge density in a crystal, and therefore it can be considered as a measure of the ''size'' of an atom in the crystal,[19] and second, the crystal inner potential is proportional to the diamagnetic susceptibility,[20] provided that magnetic interactions between ions can be neglected. It should be pointed out that by using Eq. (2) we have implicitly assumed that the crystal ionicity is an atomic quantity, and the derived crystal inner potential is therefore a bulk value which is independent of the specific surface on which our experiment was carried out. While it is true that the existence of a surface dipole layer may affect experimental RHEED intensities, our experiment was carried out under a systematic reflection geometry using relatively large angle of incidence. Since under this diffraction geometry the surface penetration depth is many times the atomic layer spacing parallel to the surface, we do not therefore expect that our measurement will be affected to any large extent by localized surface effects such as those due to the lattice relaxation near the surface.

Alternatively, the crystal inner potential may be found from Snell's refraction law.[21] For high-energy electron diffraction, this gives[22]

$$n=\frac{\lambda_0}{\lambda}=\frac{\cos\theta_0}{\cos\theta}, \tag{3}$$

in which n is the usual refraction index, λ_0 and λ denote the electron wavelength in the vacuum and in the crystal, and θ_0 and θ refer to the surface grazing angle of the specular diffracted beam in the vacuum and in the crystal, respectively. For a given energy E the electron wavelength is given by $\lambda=0.387\,831\,4/\sqrt{E(1+0.978\,467\,07\times10^{-3}E)}$, where E is expressed in keV and the electron wavelength is in Å. For a given primary beam energy of E_0 and a given crystal inner potential, V_0, $E=E_0$ in the vacuum and $E=E_0+V_0$ in the crystal. Experimentally, we can identify Bragg peaks in a RHEED pattern, and measure the angles associated with these peaks, i.e., determine the angles θ_0. For these Bragg peaks θ is simply the value given by Bragg's law being satisfied by the waves inside the crystal. For a given crystal lattice constant we may therefore solve Eq. (3) and obtain the value of the inner potential.

For low-energy electron diffraction, when the electron velocity is small in comparison with the speed of light, we may neglect relativistic effects and obtain from Eq. (3) $V_0=E\{(\cos\theta_0/\cos\theta)^2-1\}$. However for high-energy electrons, such as those of 200 keV, the electron velocity is very close to the speed of light, and relativistic effects cannot usually be neglected.

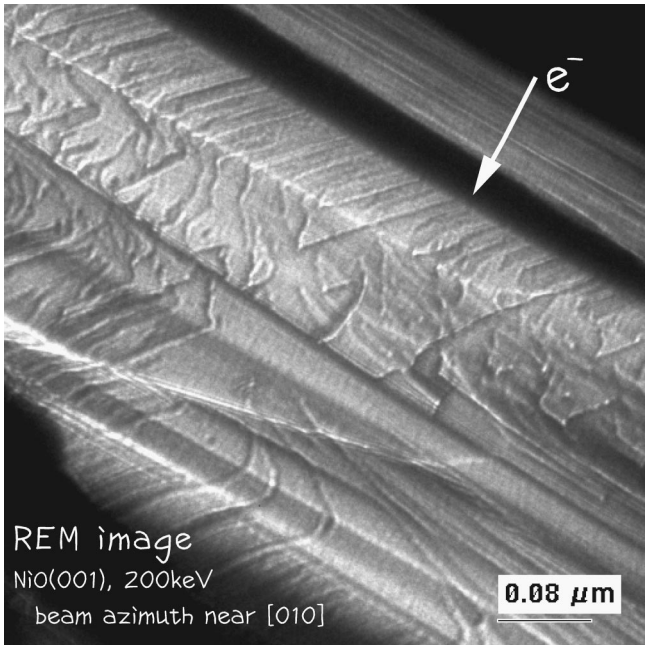

FIG. 1. REM image of a NiO(001) surface. The image was obtained for a 200-keV primary beam energy using a Philips CM200/FEG electron microscope, and the beam azimuth is near the [010] zone axis.

II. EXPERIMENTAL PROCEDURE

All RHEED and REM experiments were carried out in a field-emission gun (FEG) electron microscope (Philips CM200/FEG). The electron microscope was operated at 200 kV. NiO crystals used in this study were grown from analar materials (impurity content below 10 ppm) by K & R Creations, Japan, and the crystals were kindly provided by Dr. M. R. Castell. The specimens for RHEED and REM observations were prepared by cleavage along the (001) faces. The sample size was $1\times1\times0.2$ mm.[3]

NiO crystals have the rocksalt structure with a lattice constant of $a_0=4.168$ Å. REM observations of the cleavage (001) surface of NiO reveal that the surface is in general flat, and in some regions the surface is atomically flat, with a low density of surface defects such as surface steps and dislocations. Figure 1 is a REM image of the (001) surface, showing that the area under examination is atomically flat over a dimension of at least a few micrometers. The RHEED pattern recorded for quantitative studies was obtained from an atomically flat region. It should be pointed out that for a REM image there exist two scales. The scale shown in Fig. 1 is the normal scale which characterizes the dimension perpendicular to the incident beam direction. On the other hand, the image is severely foreshortened in the beam direction.

TABLE I. Parametrization of the real part of the atomic scattering factors.

	a_1	a_2	a_3	a_4	a_5	b_1	b_2	b_3	b_4	b_5
Ni^{2+}	0.0607	0.2064	0.6276	1.2043	0.6011	0.0373	0.2556	1.1269	3.5840	12.2437
O^{2-}	0.0421	0.2104	0.8517	1.8177	1.1739	0.0609	0.5592	2.9559	11.4851	37.6780
N	0.3860	1.1765	1.5451	2.0730	1.3814	0.2478	1.7660	6.3107	25.220	74.315
O	0.0974	0.2921	0.6910	0.6990	0.2039	0.2067	1.3815	4.6943	12.711	32.473

TABLE II. Parametrization of the imaginary part of the atomic scattering factors.

	a_1	a_2	a_3	a_4	a_5	b_1	b_2	b_3	b_4	b_5
Ni	0.1953	3.2064	−11.3924	12.7914	−4.7039	2.0100	11.9912	13.9906	16.3106	19.6967
O	0.0190	7.2509	−45.0028	46.9728	−9.2302	2.0186	13.8727	15.0867	15.6324	16.9602

The scale along this direction (not shown in the figure) is 36 times shorter than the normal scale shown in the figure. The atomically flat area shown in Fig. 1 is therefore approximately 15 micrometers along the beam direction, and 0.5 micrometers perpendicular to the beam direction.

III. ATOMIC SCATTERING FACTOR

The atomic scattering factors for both the neutral atoms and ions of Ni and O have been calculated by Doyle and Turner,[23] and more recently by Rez, Rez, and Grant.[24] For dynamical RHEED calculations it is convenient to fit the atomic scattering factors to a linear combination of Gaussians,[25]

$$f(s)=\sum_{i=1}^{5} a_i \exp(-b_i s^2)+\frac{me^2}{2h^2}\frac{\Delta Z}{s^2}, \tag{4}$$

in which ΔZ is the ionic charge. For the Ni^{2+} ion we assumed that $\Delta Z=2$, and for the O^{2-} ion $\Delta Z=-2$. For all the elements of the Periodic Table the parameters for the real part of the atomic scattering factors of neutral atoms were tabulated by Peng *et al.*[26] For the ions of interest here, these parameters were obtained following the procedure outlined in Ref. 26, and are given in Table I.

The imaginary part of the atomic scattering factor may be calculated following the standard procedure,[27–29] assuming that lattice vibrations are isotropic. This imaginary part depends on the primary beam energy and on the temperature B factors. In the present study the temperature factor B for the Ni atom is taken from Ref. 30, calculated for the elemental Ni single crystal, and that for O was assumed to be the same as for MgO, for which an accurate B factor has been determined using convergent-beam electron diffraction.[31] These B factors are 0.315 $Å^2$ for O and 0.356 $Å^2$ for Ni. Using these values, we calculated the imaginary part of the atomic scattering factors for neutral atoms of Ni and O and for a range of s values. These values were then fitted by a sum of the Gaussians as in Eq. (4). Table II gives the parameters for a 200-keV primary beam energy. For ions these values are slightly different, but for the purpose of the present study we used the same parameters for ions.

IV. RESULTS AND DISCUSSIONS

RHEED patterns normally show sensitivity to a number of parameters, including the detailed surface structure and the temperature factor. In the present study we are primarily concerned with the crystal ionicity and inner potential, which are parameters characterizing bulk properties of the material rather than its surface properties. Therefore the experiments were performed using systematic Bragg diffraction geometry, for which surface resonance effects are minimized and the penetration depth of the primary beam is relatively large.[32]

In Fig. 2 is shown an experimental RHEED pattern taken from the (001) surface of a single crystal of NiO using a beam of energy 200 keV. The beam is incident at the surface at an azimuth which is a few degrees away from the main [010] zone axis. It is seen that around the central region this RHEED pattern is dominated by the horizontal Kikuchi lines, suggesting that the diffraction processes are mainly those systematic interactions involving planes parallel to the (001) surface. At least six horizontal Kikuchi lines can be easily identified in the pattern. The line which is nearest to the shadow edge has an index of (4,0,0). The indices of the other lines are (6,0,0), (8,0,0), (10,0,0), (12,0,0) and (14,0,0), respectively.

The RHEED pattern shown in Fig. 2 is primarily a Kikuchi pattern, and most of the contrast features are generated by dynamical diffraction processes of the diffusely scattered electrons.[33] The positions of the Kikuchi lines may, however, be related to the Bragg peak positions of the elastic dynamical RHEED rocking curves.[34] Therefore in this study we will use the usual RHEED rocking curve calculated using dynamical RHEED theory to obtain the Bragg peak positions, and to compare these positions with the measured experimental horizontal Kikuchi line positions.[32]

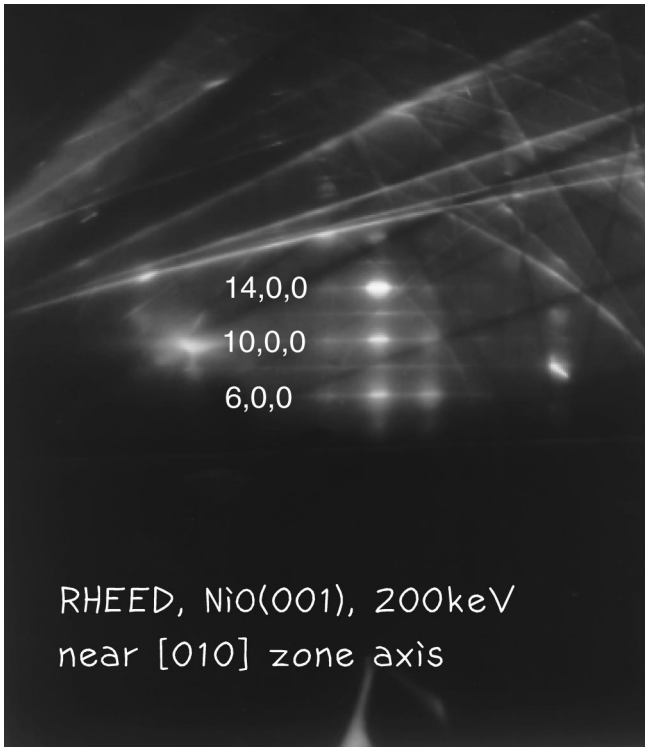

FIG. 2. Experimental RHEED pattern from the NiO(001) surface. The primary beam energy is 200 keV, and the electrons are incident at the surface near the [010] zone axis.

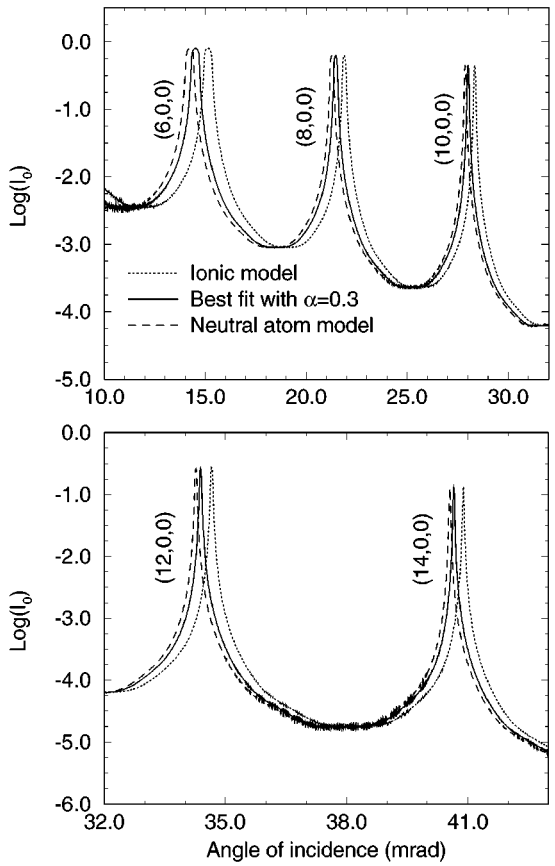

FIG. 3. Systematic RHEED rocking curves calculated for the NiO(001) surface, using a neutral atom model with $\alpha=0$ (solid line) and an ionic model with $\alpha=1$ (dotted line). The B factors used in the calculations are 0.315 Å^2 for O and 0.356 Å^2 for Ni. The logarithms are base 10.

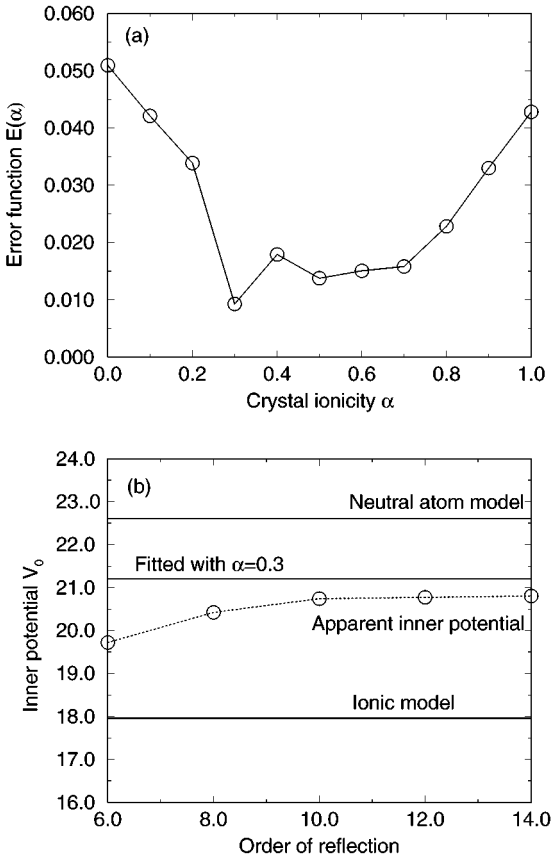

FIG. 4. (a) The error factor E as a function of crystal ionicity. (b) Apparent crystal inner potential as a function of the order of reflections.

Shown in Fig. 3 are three calculated RHEED rocking curves for a systematic reflection geometry. These rocking curves were calculated for a 200-keV primary beam energy and the (001) surface of a NiO single crystal, and the three curves correspond to a neutral atom model with $\alpha=0$ (dashed line), an ionic model with $\alpha=1$ (dotted line), and an intermediate model with $\alpha=0.3$ (solid line), respectively. This figure clearly shows that for all reflections, in particular lower order reflections, such as (600) and (800), the shifts in peak positions between the three curves are well distinguishable. The effect of temperature B factor on RHEED rocking curve has also been investigated. RHEED rocking curves were calculated using different temperature B factors, and it was found that to a very good approximation the temperature B factors affect the absolute intensity rather than the peak position.

To measure the Kikuchi line positions accurately, the experimental RHEED pattern shown in Fig. 2 was first scanned into the computer using a 600-dpi scanner with a resolution of 2700×3300. Horizontal Kikuchi lines of (6,0,0), (8,0,0), (10,0,0), (12,0,0), and (14,0,0) were then fitted into a set of straight lines using the Gatan image processing software Digital Micrograph, and distances between these lines were measured with an accuracy of better than 1%. Shown in Table III are measured line distances d_h, each defined as the distance between the (h,0,0) and (6,0,0) horizontal Kikuchi lines, and the ratios r_h which are given by $r_h=d_h/d_8$.

TABLE III. Measured distances and ratios for horizontal Kikuchi lines.

Line index	(8,0,0)	(10,0,0)	(12,0,0)	(14,0,0)
d	102.08	198.16	293.24	387.33
r	1.0	1.9402	2.8726	3.7944

For a given crystal ionicity α, we may obtain the atomic scattering factor using Eq. (1) and calculate the corresponding RHEED rocking curve. To measure the goodness of fitting of a calculated RHEED rocking curve to the experimental RHEED pattern, we define an error factor E,

$$E(\alpha)=\{(r_{10}^{\alpha}-r_{10}^{\mathrm{expt}})^2+(r_{12}^{\alpha}-r_{12}^{\mathrm{expt}})^2+(r_{14}^{\alpha}-r_{14}^{\mathrm{expt}})^2\}^{1/2}, \tag{5}$$

in which the superscripts α and expt refer to the calculated r values for a given α and that of the experimental measurements, and the subscript on r denotes the order of reflections.

Shown in Fig. 4(a) is a plot of the error factor E as against the crystal ionicity α. The plot shows clearly a minimum at $\alpha\approx0.3$ and the E factor increases rapidly toward $\alpha=0$ and 1. We therefore conclude that the single crystal of NiO is composed of constituents which are neither neutral atoms nor ions. However, our result indicates that the constituents

are closer to neutral atoms than to ions, and this conclusion is in agreement with the Mattheiss' conjecture[12] that a consistent *ab initio* solution may be reached faster starting from neutral atom wave functions rather than from those of individual ions.

For a given α the crystal inner potential may be calculated using Eq. (2). Using the parameters given in Table I, we obtain $V_0 = 22.6034$ V for the neutral atom model and $V_0 = 7.9585$ V for the ionic model. For $\alpha = 0.3$ we obtain $V_0 = 21.21$ V.

Alternatively an apparent inner potential may be calculated from the Bragg peak position by solving Eq. (3). For $\alpha = 0.3$ we obtain the inner potential as a function of the order of reflections, and the results are shown in Fig. 4(b). It is seen that the error is larger for lower-order reflections, while for higher-order reflections the deviation from the exact value is within 0.5 V. The variation in the measured crystal inner potential for different orders of reflections is due to the fact that, in deriving Snell's law (3), we assumed that the incident electron is scattered only by the crystal inner potential V_0, i.e., the effect of all other Fourier coefficients of the crystal potential is neglected. For small angle of incidence the effect due to other V_g's is expected to be strong, while for large angles of incidence this effect is usually weaker.

In the present treatment the charge distribution associated with each ion was implicitly assumed to be spherically symmetric. In a real crystal, however, the distribution of charge associated with each lattice site is expected to deviate from spherical symmetry. Since this deviation affects largely the low rather than high frequency components of V_g and therefore it should mostly influence the low-angle region of RHEED rocking curves,[35,36,17] its effect is minimized in the presented study where we used only the large-angle region of the RHEED rocking curve.

V. CONCLUSIONS

The techniques of RHEED and REM have been applied to a study of the NiO(001) surface. REM observation shows that the cleavage (001) surface of the NiO crystal is usually flat, and in some regions the surface can be atomically flat, having a low density of surface defects. RHEED patterns obtained from an atomically flat region were compared with dynamical RHEED calculations. The crystal ionicity and the inner potential of the NiO single crystal are determined to be about 0.3 and 21.21 V, respectively, by quantitative fitting of theoretical calculations to the experimental measurements.

ACKNOWLEDGMENTS

We are grateful to M. R. Castell, J.-M. Zuo, J. C. H. Spence, and A. P. Sutton for stimulating discussions. This work was supported by the National Natural Science Foundation of China (Grant No. 19425006), K. C. Wong Education Foundation, and by the Chinese Academy of Sciences and the Royal Society via a joint project (Project No. Q711). We gratefully acknowledge financial support from these bodies.

[1] V. E. Henrich and P. A. Cox, *The Surface Science of Metal Oxides* (Cambridge University Press, Cambridge, 1994).
[2] C. Noguera, *Physics and Chemistry at Oxide Surfaces* (Cambridge University Press, Cambridge, 1996).
[3] V. F. Kiselev and O. V. Krylov, *Adsorption and Catalysis on Transition Metals and Their Oxides* (Springer-Verlag, New York, 1989).
[4] S. Hüfner, Adv. Phys. **43**, 183 (1994).
[5] A. Georges, G. Kotliar, W. Krauth, and M. J. Rozenberg, Rev. Mod. Phys. **68**, 13 (1996).
[6] M. D. Towler, N. L. Allan, N. M. Harrison, V. R. Saunders, W. C. Mackrodt, and E. Apra, Phys. Rev. B **50**, 5041 (1994).
[7] O. Tjernberg, S. Söderholm, G. Chiaia, R. Girard, U. O. Karlsson, H. Nylén and I. Lindau, Phys. Rev. B **54**, 10 245 (1996).
[8] K. Doll, M. Dolg, P. Fulde, and H. Stoll, Phys. Rev. B **55**, 10 282 (1997).
[9] M. R. Castell, P. L. Wincott, N. G. Condon, C. Muggelberg, G. Thornton, S. L. Dudarev, A. P. Sutton, and G. A. D. Briggs, Phys. Rev. B **55**, 7859 (1997).
[10] S. L. Dudarev, A. I. Liechtenstein, M. R. Castell, G. A. D. Briggs, and A. P. Sutton, Phys. Rev. B **56**, 4900 (1997).
[11] W. Reichardt, V. Wagner, and W. Kress, J. Phys. C **8**, 3955 (1975).
[12] L. F. Mattheiss, Phys. Rev. B **5**, 290 (1972).
[13] D. D. Vvedensky and J. B. Pendry, Surf. Sci. **152/153**, 33 (1985).
[14] J. C. H. Spence and J. M. Zuo, *Electron Microdiffraction* (Plenum, New York, 1992).
[15] R. M. Stern and A. Gervais, Surf. Sci. **17**, 273 (1969).
[16] G. P. Thomson and W. Cochrane, *Theory and Practice of Electron Diffraction* (Macmillan, London, 1939).
[17] J. C. H. Spence, Acta Crystallogr., Sect. A: Found. Crystallogr. **49**, 231 (1993).
[18] M. O'Keeffe and J. C. H. Spence, Acta Crystallogr., Sect. A: Found. Crystallogr. **50**, 33 (1994).
[19] H. A. Bethe, Ann. Phys. (Leipzig) **87**, 55 (1928).
[20] S. Miyake, Proc. Phys. Math. Soc. Jpn. **22**, 666 (1940).
[21] M. Born and E. Wolf, *Principles of Optics*, 6th ed. (Pergamon, Oxford, 1980).
[22] P. B. Hirsch, A. Howie, R. N. Nicholson, D. W. Pashley, and M. J. Whelan, *Electron Microscopy of Thin Crystals* (Krieger, Malabar, 1977).
[23] P. A. Doyle and P. S. Turner, Acta Crystallogr., Sect. A: Cryst. Phys., Diffr., Theor. Gen. Crystallogr. **24**, 390 (1968).
[24] D. Rez, P. Rez, and I. Grant, Acta Crystallogr., Sect. A: Found. Crystallogr. **50**, 481 (1994).
[25] S. L. Dudarev, M. J. Whelan, and L.-M. Peng Surf. Sci. **330**, 86 (1995).
[26] L.-M. Peng, G. Ren, S. L. Dudarev and M. J. Whelan, Acta Crystallogr., Sect. A: Found. Crystallogr. **52**, 257 (1996).
[27] C. R. Hall and P. B. Hirsch, Proc. R. Soc. London, Ser. A **286**, 177 (1965).
[28] C. J. Rossouw and L. A. Bursill, Acta Crystallogr., Sect. A: Found. Crystallogr. **41**, 320 (1985).
[29] D. M. Bird and Q. A. King, Acta Crystallogr., Sect. A: Found. Crystallogr. **46**, 202 (1990).
[30] L.-M. Peng, G. Ren, S. L. Dudarev, and M. J. Whelan, Acta

Crystallogr., Sect. A: Found. Crystallogr. **52**, 456 (1996).
[31] L.-M. Peng and J. M. Zuo, Ultramicroscopy **57**, 1 (1995).
[32] L.-M. Peng and M. J. Whelan, Proc. R. Soc. London, Ser. A **432**, 195 (1991).
[33] J. M. Cowley, *Diffraction Physics*, 2nd ed. (North-Holland, Amsterdam, 1990).
[34] J. Gjønnes, A. Olsen, and H. Matsuhata, J. Electron Microsc. Technol. **13**, 98 (1989).
[35] D. J. Smart and C. J. Humphreys, Inst. Phys. Conf. Ser. **52**, 211 (1980).
[36] J. M. Zuo, J. C. H. Spence, and M. O'Keeffe, Phys. Rev. Lett. **61**, 353 (1988).